Magneto-Optical Investigations of Imidogen in Inert-Gas Matrices

Jeremy J. Harrison[†] and Bryce E. Williamson*

Department of Chemistry, University of Canterbury, Private Bag 4800, Christchurch, New Zealand

Janna L. Rose

Rayovac Corporation, 601 Rayovac Drive, Madison, Wisconsin 53711

Received: November 12, 2003; In Final Form: January 29, 2004

Magnetic circular dichroism (MCD) and absorption spectra are reported for the A $^3\Pi_i \leftarrow$ X $^3\Sigma^-$ transition of imidogen (NH) isolated in Kr, Xe, and N_2 matrices at cryogenic temperatures (∼1.4−20 K) and over a range of magnetic field strengths (0−5 T). The results are analyzed by the method of moments, and parameters are extracted by fitting the experimental data to a model in which the A $^3\Pi_i$ term is split by spin−orbit (SO) coupling interactions and the X $^3\Sigma^-$ term is split by spin−spin and higher-order SO coupling. The analysis indicates that the ground-state NH radicals behave essentially as free rotors in the noble-gas matrices but as hindered rotors in solid N_2. Trends in excited-state SO coupling constants are attributed to the external heavy-atom effect.

I. Introduction

This paper is a sequel to one published in 1998 concerning the magnetic circular dichroism (MCD) and absorption spectroscopy of the imidogen (NH) radical isolated in solid Ar (NH/Ar).[1] The work reported here extends measurements to NH/Kr, NH/Xe, and NH/N_2 with the aim of determining and rationalizing trends that pertain to guest−host interactions and the dynamics of the guest radical.[2]

A detailed review of previous spectroscopic investigations of NH was provided in the earlier paper.[1] Here we summarize only the literature pertaining to the matrix-isolated species.

Spectra of NH isolated in noble-gas (NG = Ar, Kr, and Xe) matrices were first reported in 1958 by Robinson and McCarty.[3,4] The same workers later concluded that NH undergoes essentially free rotation in solid Ar.[5] In 1975, Bondybey and Brus reported laser-induced fluorescence and vibrational relaxation for NH and ND in Ar and Kr,[6] also concluding that the guest radicals undergo essentially free rotation in the ground state but that rotations are strongly hindered in the excited state.

In 1982, Lund et al. were the first to report MCD data for NH/Ar and NH/Xe.[7] Five years later, Rose reported the MCD of NH/Ar and NH/Xe over a range of temperatures and magnetic field strengths, which she attempted to interpret within the framework of a free-rotor model.[8]

Our earlier work concerned a detailed examination of the MCD and absorption spectra of NH/Ar and ND/Ar over the temperature range of 1.6−16 K and for magnetic fields up to 4.5 T.[1,9] We were able to interpret the results in terms of a spin−orbit crystal-field (SO−CF) model, developed previously for the interpretation of OH/Ar[9,10] and CH/Ar[9,11] data. The conclusions from this previous work are in agreement with those of Bondybey and Brus[6]—that ground-state NH in solid Ar undergoes free rotation, whereas the excited-state radicals depart strongly from free rotation. The former result was evidenced by the strong quenching of the zero-field splitting, whereas the second was accompanied by excited-state SO and CF splitting parameters of $A_\Pi = -33.5$ cm^{-1} and $V_0 \approx 38$ cm^{-1}, respectively.

Having obtained independent information to support the hypothesis that ground-state NH is effectively a free rotor in Ar, we now report similar investigations of NH/Kr and NH/Xe. To test the sensitivity of our approach, data were also obtained for NH/N_2 because of prior evidence that guest rotation is strongly hindered in matrices (such as N_2) with unsymmetrical trapping sites.[12]

II. Experimental Section

MCD (ΔA) and double-beam absorption (A) spectra were measured simultaneously by using a spectrometer[9,10] equipped with a Xe-arc lamp, a 1180-groove/mm grating blazed at 300 nm, and a Hamamatsu R-376 PMT. A Corning 7-54 filter was used to remove stray visible light prior to the sample, and the spectral resolution was 0.2 nm (∼20 cm^{-1}).

Samples were prepared from anhydrous NH_3 (Matheson) mixed with Kr, Xe (Linde), or N_2 (BOC) to a pressure of ∼1 atm at mole ratios of ∼1:100. NH radicals were produced by subjecting the mixture to a Tesla-coil discharge as it flowed at ∼2−3 mmol h^{-1} through a 12-mm (i.d.) Pyrex or quartz tube. The products were deposited for 30 to 60 min onto a *c*-cut sapphire sample window held at a temperature below 20 K.

Preliminary experiments to determine optimum sample preparation conditions were performed using an APD Cryogenics Inc. closed-cycle He refrigerator placed between the poles of an Alpha Magnetics Inc. 4800 electromagnet.[9,10] Subsequent experiments were conducted using a matrix-injection system consisting of an Oxford Instruments SM4 magneto-cryostat, a matrix-deposition chamber, and a siphon rod, the tip of which contains a sapphire window.[13,14] Temperatures above 4.2 K were monitored by using a calibrated carbon resistance thermometer, and lower temperatures, down to ∼1.4 K, were obtained by pumping the vapor above the liquid and were determined by measuring the pressure with a capacitance manometer.[15]

Good yields of NH were obtained for all three host gases using the He-refrigerator/electromagnet setup. However, for

* Corresponding author. E-mail: bryce.williamson@canterbury.ac.nz. Fax: ++ 64 3 364 2110. Tel: ++ 64 3 364 2439.

[†] Present addresses: Institut für Physikalische Chemie, Georg-August-Universität Göttingen, Tammannstrasse 6, 37077 Göttingen, Germany, and Max-Planck-Institut für Biophysikalische Chemie, Am Fassberg 11, 37077 Göttingen, Germany.

10.1021/jp0374556 CCC: $27.50
Published on Web 03/16/2004

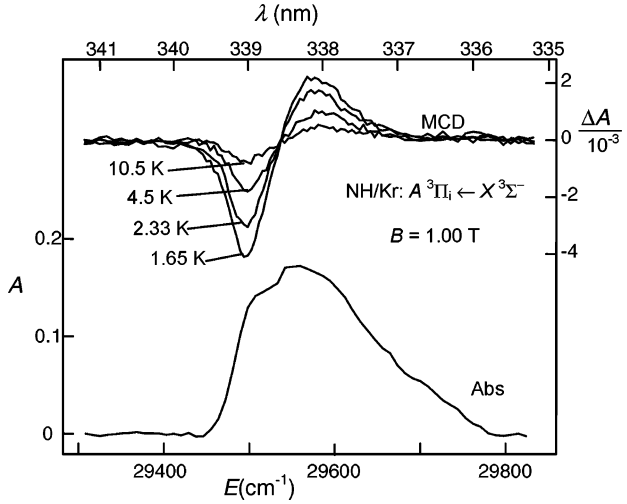

Figure 1. Absorption (bottom) and temperature-dependent MCD spectra (1.00 T) of the (0, 0) band of the A $^3\Pi_i \leftarrow$ X $^3\Sigma^-$ transition of NH/Kr.

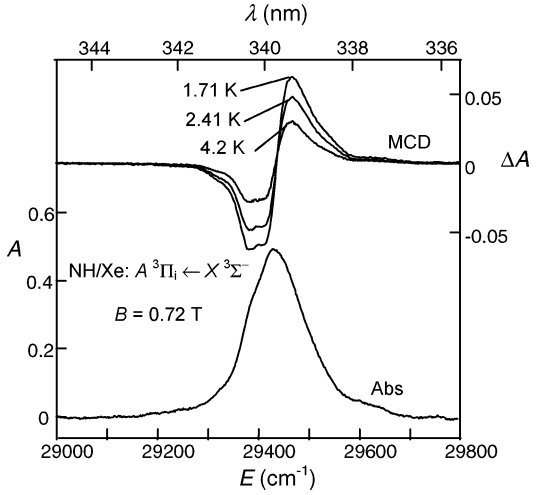

Figure 2. Absorption (bottom) and temperature-dependent MCD spectra (0.72 T) of the (0, 0) band of the A $^3\Pi_i \leftarrow$ X $^3\Sigma^-$ transition of NH/Xe (original data from ref 8).

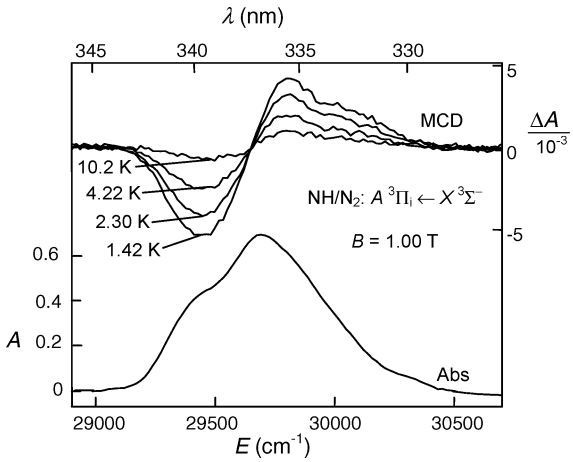

Figure 3. Absorption (bottom) and temperature-dependent MCD spectra (1.00 T) of the (0, 0) band of the A $^3\Pi_i \leftarrow$ X $^3\Sigma^-$ transition of NH/N_2.

reasons that could not be ascertained, the quality of the NH/Kr and, particularly, the NH/Xe spectra was severely worse when using the matrix-injection equipment. For NH/Xe, we resorted to data obtained in 1985 at the University of Virginia[8] using the same preparation methods but with earlier versions of the spectrometer[16,17] and matrix-injection system.[18,19]

III. Results

MCD and its origins are described in detail by Piepho and Schatz.[20] It is quantified by ΔA, the difference between the absorbance of left and right circularly polarized light by a sample in the presence of a longitudinal magnetic field, and A is the corresponding average:[20]

$$\Delta A = A_{\mathrm{lcp}} - A_{\mathrm{rcp}} \tag{1}$$

$$A = \frac{A_{\mathrm{lcp}} + A_{\mathrm{rcp}}}{2} \tag{2}$$

An appropriate comparison of ΔA and A permits the determination of ground- and excited-state electronic angular momenta, even when transition bandwidths are very much greater than the Zeeman shifts. MCD is therefore a valuable technique for dealing with molecules and has proved very useful for probing, for example, vibronic and environmental effects through their interactions with those angular momenta.

The features observed in MCD spectra are categorized as Faraday $\mathscr{A}$, $\mathscr{B}$, and $\mathscr{C}$ terms.[20] $\mathscr{A}$ terms are derivative-shaped, temperature-independent, and arise from first-order Zeeman splittings of the ground state and/or the excited state. $\mathscr{B}$ terms are single-signed (positive or negative), temperature-independent, and arise from the higher-order magnetic field-induced mixing of states. They are generally weak except when the energy difference between the interacting states is small. Single-signed (positive or negative) and temperature-dependent $\mathscr{C}$ terms arise from population differences between the Zeeman-split levels of the ground electronic state. For systems (such as NH) with paramagnetic ground states, $\mathscr{C}$ terms usually dominate. Unlike $\mathscr{A}$ and $\mathscr{B}$ terms, whose magnitudes scale linearly with the applied magnetic field, $\mathscr{C}$ terms exhibit magnetization saturation behavior as the temperature is lowered and/or the magnetic field strength is increased.

The absorption and the temperature dependence of the MCD spectra for the (0, 0) bands of the A $^3\Pi_i \leftarrow$ X $^3\Sigma^-$ transitions of the three samples are shown in Figures 1−3. The MCD spectra show a double-signed dispersion with the negative lobe at lower energy, as observed previously for NH/NG.[1,7−9] This type of appearance is normally attributed to positive $\mathscr{A}$ terms. However, the observed temperature dependence, as well as the fact that the MCD exhibits saturation at high magnetic field strengths (as shown for NH/Kr in Figure 4), indicates that the spectra are actually dominated by pairs of $\mathscr{C}$ terms of opposite sign.[1]

As the atomic number of the noble-gas host atoms is increased, the bands show an increasing bathochromic shift, in accordance with previous observations for molecules trapped in noble-gas matrices.[21] They also become more diffuse and less structured. For NH/N_2, the (0, 0) band is very much broader than for any of the noble-gas systems, suggesting the presence of much stronger guest−host interactions.

The intensities of the spectra were quantified by using moment analysis;[20] the nth absorbance and MCD moments are, respectively,

$$\mathbf{A}_n = \int_{\mathrm{band}} \frac{A(E)}{E} (E - \bar{E})^n \, \mathrm{d}E \tag{3}$$

$$\mathbf{M}_n = \int_{\mathrm{band}} \frac{\Delta A(E)}{E} (E - \bar{E})^n \, \mathrm{d}E \tag{4}$$

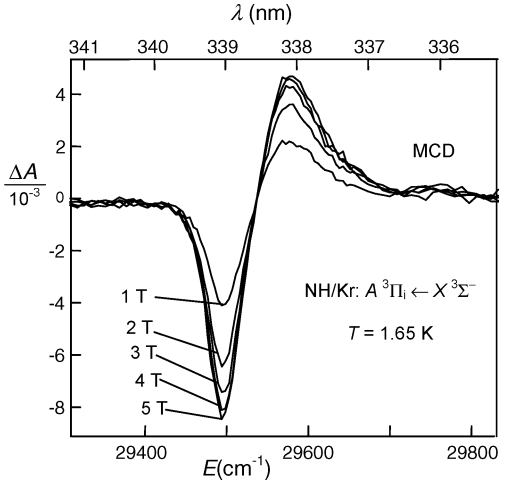

Figure 4. Magnetic field-dependent MCD spectra (1.65 K) of the (0, 0) band of the A $^3\Pi_i \leftarrow$ X $^3\Sigma^-$ transition of NH/Kr.

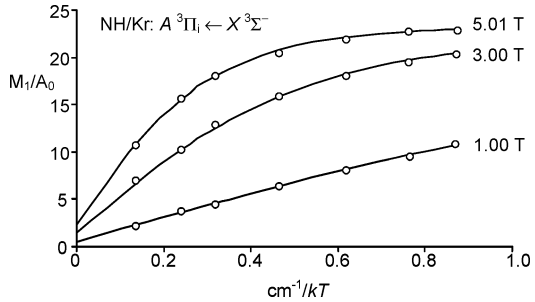

Figure 5. Temperature dependence of the moment ratio $\mathbf{M}_1/\mathbf{A}_0$ as a function of $1/kT$ for the (0, 0) band of the A $^3\Pi_i \leftarrow$ X $^3\Sigma^-$ transition of NH/Kr. The curves are best fits to all data using eq 7, with $A_\Pi = -21$ cm^{-1} and $D' = 0$ cm^{-1}.

TABLE 1: Barycenters and Bandwidths for the (0, 0) Bands of the A $^3\Pi \leftarrow$ X $^3\Sigma^-$ Systems of Matrix-Isolated NH

matrix	$\bar{E}$/cm^{-1}	$2\sqrt{\mathbf{A}_2/\mathbf{A}_0}$/cm^{-1}
NH/Ar	29 670	130
NH/Kr	29 550	130
NH/Xe	29 430	140
NH/N_2	29 710	500

Here, E is the photon energy, $\bar{E}$ is the absorption band barycenter (the average energy defined by the requirement that $\mathbf{A}_1 = 0$), and the integrals are carried out over the full envelope of the transition. The $\bar{E}$ values and effective bandwidths, $2\sqrt{\mathbf{A}_2/\mathbf{A}_0}$, for the (0, 0) bands are collected in Table 1.

For the analysis that follows, $\mathbf{M}_1/\mathbf{A}_0$ was evaluated numerically for each spectrum. This ratio has the advantage that it is independent of variables such as transition moments and the concentration, path length, and refractive index of the sample. It is also invariant to unitary transformations of the excited-state basis,[20] which allows simpler expressions to be developed for analysis. However, the offsetting disadvantage is that it provides no direct information about the details of excited-state CF interactions.

$\mathbf{M}_1/\mathbf{A}_0$ ratios for various magnetic field strengths are plotted against $1/kT$ in Figures 5−7. The high-field data for NH/Kr and NH/N_2 (Figures 5 and 7, respectively) show obvious saturation. Those for NH/Xe (Figure 6) were collected over a narrower magnetic field range, and saturation is less clearly apparent.

IV. Discussion

The A $^3\Pi_i \leftarrow$ X $^3\Sigma^-$ system of NH arises from the $1\pi \leftarrow 3\sigma$ excitation, where the 1π orbitals are nonbonding N $2p_{\pm1}$ and

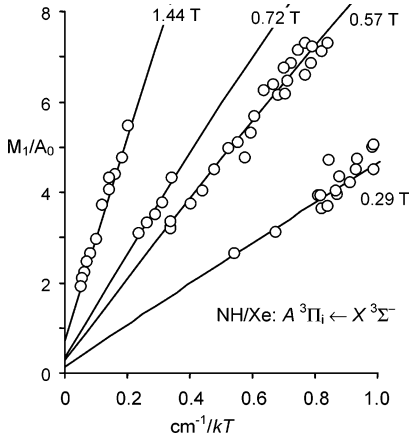

Figure 6. Temperature dependence of the moment ratio $\mathbf{M}_1/\mathbf{A}_0$ as a function of $1/kT$ for the (0, 0) band of the A $^3\Pi_i \leftarrow$ X $^3\Sigma^-$ transition of NH/Xe (original data from ref 8). The curves are best fits to all data using eq 7, with $A_\Pi = -25.6$ cm^{-1} and $D' = 0$ cm^{-1}.

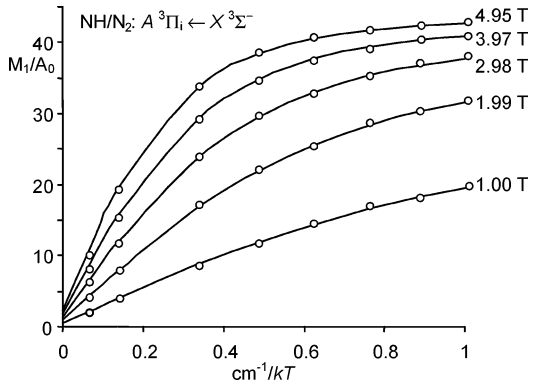

Figure 7. Temperature dependence of the moment ratio $\mathbf{M}_1/\mathbf{A}_0$ as a function of $1/kT$ for the (0, 0) band of the A $^3\Pi_i \leftarrow$ X $^3\Sigma^-$ transition of NH/N_2. The curves are best fits to all data using eq 7, with $A_\Pi = -43.2$ cm^{-1} and $D' = 0.61$ cm^{-1}.

3σ is an admixture mainly of N $2p_0$ with H 1s. In the excited term, the spin and orbital angular momenta are strongly coupled to the internuclear axis, and the electronic states are described in a Hund's case (a) basis, $|^3\Pi_{|\Omega|}\ \Lambda\ \Sigma\rangle$; $\Sigma = 0, \pm1$ and $\Lambda = \pm1$ denote, respectively, the projections of the electronic spin and orbital angular momenta along the internuclear axis, and Ω is the sum of Λ and Σ. SO interactions give rise to three levels quantized by $|\Omega| = 0$, 1, and 2. Ignoring the much weaker spin−spin (SS) and higher-order SO effects, the energies are

$$E(^3\Pi_{|\Omega|}) = T_\Pi + A_\Pi(|\Omega| - 1) \qquad (5)$$

In the gas phase, the electronic term value and the SO coupling constant are, respectively, $T_\Pi \approx 29\,810$ cm^{-1} and $A_\Pi = -34.79$ cm^{-1}.[22] On incorporation of the radical into a condensed medium, eq 5 still holds but with T_Π and A_Π taking modified values.

For the unconstrained ground-state NH radical, the spin is not coupled to the internuclear axis. The X $^3\Sigma^-$ term therefore belongs to Hund's case (b) and is not split by first-order SO (or CF) effects. Higher-order SO (predominantly involving the b $^1\Sigma^+$ term from the same configuration) and SS interactions cause a zero-field splitting (ZFS), denoted D, which is not evident in the lowest ($J = 1$) free-rotor level but becomes apparent at higher rotational levels.

When the radical is rotationally constrained, higher-order interactions permit the spin to couple to the internuclear axis in the X $^3\Sigma^-$ term, and it is more convenient to treat the

TABLE 2: Hamiltonian Matrix for the X $^3\Sigma^-$ Term of NH

	$\|^3\Sigma_1^- -1\rangle$	$\|^3\Sigma_0^- 0\rangle$	$\|^3\Sigma_1^- +1\rangle$
$\langle^3\Sigma_1^- -1\|$	$D'/3 - g_e\mu_B B\cos\theta$	$g_e\mu_B B\sin\theta/\sqrt{2}$	0
$\langle^3\Sigma_0^- 0\|$	$g_e\mu_B B\sin\theta/\sqrt{2}$	$-2D'/3$	$-g_e\mu_B B\sin\theta/\sqrt{2}$
$\langle^3\Sigma_1^- +1\|$	0	$-g_e\mu_B B\sin\theta/\sqrt{2}$	$D'/3 + g_e\mu_B B\cos\theta$

component states in a Hund's case (a) basis, $|^3\Sigma^-_{|\Omega|}\ \Sigma\rangle$, where $\Lambda = 0$ (and is omitted from the ket) and $\Omega = \Sigma = 0, \pm 1$. The level with $J = 1$ gas-phase parentage now exhibits a ZFS with energies of

$$E(^3\Sigma^-_{|\Omega|}) = \left(\left|\Omega\right| - \frac{2}{3}\right)D' \qquad (6)$$

D' is an effective ZFS parameter.

For a stationary guest radical in a "noninteracting" host, D' would be close to the gas-phase value of D. However, in real situations it can be substantially modified by matrix effects. First, the influence of nearby host atoms can alter the SO contribution to the ZFS. Second, if the facility of guest rotation is increased, then the spin is progressively decoupled from the internuclear axis, and D' will approach zero (the free-rotor condition of a degenerate $J = 1$ level), an effect that is referred to as motional averaging.[23]

EPR is normally the preferred technique for measuring ground-state ZFSs for paramagnetic species. However, EPR experiments performed on NH/NG matrices have proved fruitless, partly as a result of the congestion of the spectra by other radical species produced in the discharge processes. In our earlier work, we have shown that MCD provides an alternative method,[1] with the advantage that A $^3\Pi_i \leftarrow$ X $^3\Sigma^-$ is well separated from the electronic transitions of other species, thereby circumventing the congestion problem.

A detailed account of the theoretical basis of our approach has been presented previously.[1] Starting from the assumption that the guest radicals are stationary but randomly oriented in the matrix, it yields

$$\frac{\mathbf{M}_1}{\mathbf{A}_0} = \mu_B B + \left(\frac{3A_\Pi}{2}\right)\int_{-1}^{1}\sum_i P_i(|C_{+1,i}|^2 - |C_{-1,i}|^2)\cos\theta\ \mathrm{d}\cos\theta \qquad (7)$$

The first term in eq 7 is linear in B and represents the $\mathscr{A}$-term contribution resulting from the excited-state orbital angular momentum. The second comprises contributions from $\mathscr{C}$ terms of opposite sign, which would cancel if they were not separated by excited-state SO splitting. The $C_{\Sigma,i}$ are coefficients given by

$$C_{\Sigma,i} = \langle^3\Sigma^-\ \Sigma|^3\Sigma^-\ i\rangle \qquad (8)$$

where $|^3\Sigma^-\ i\rangle$ ($i = 1, 2, 3$ in order of ascending energy) are the eigenstates of the Hamiltonian in Table 2. The saturation phenomenon enters eq 7 through the temperature and field dependencies of the Boltzmann populations, P_i. The integral over $\cos\theta$ is achieved numerically and accounts for the random orientation of the guest species.

Least-squares fits of the $\mathbf{M}_1/\mathbf{A}_0$ data using eq 7 yield the parameters listed in Table 3. The corresponding calculated magnetic field and temperature dependencies, illustrated as continuous curves in Figures 5−7, reproduce the experimental data accurately and precisely over the full ranges of temperature and magnetic field. The nonzero ordinate intercepts of each plot are a consequence of the $\mathscr{A}$-term contributions to the MCD.

TABLE 3: Parameters for the A $^3\Pi_i \leftarrow$ X $^3\Sigma^-$ Transition of NH in the Gas Phase and in Inert-Gas Matrices

matrix	NH (gas)[a]	NH/Ar[b]	NH/Kr	NH/Xe	NH/N_2
A_Π/cm^{-1}	−34.79	-33.5 ± 0.3	-21 ± 2	-25.6 ± 0.6	-43.2 ± 0.3
D'/cm^{-1}	1.67	-0.08 ± 0.03	0.01 ± 0.01	0.04 ± 0.01	0.61 ± 0.02

[a] From refs 22 and 31. D' is equated to the gas-phase ZFS, which is not manifest as a zero-field splitting of the lowest ($J = 1$) level of the X $^3\Sigma^-$ state. [b] From ref 1.

TABLE 4: One-Electron SOC Constants (cm^{-1}) for the ^{2}P Terms of Metals and the A $^3\Pi_i$ Term of NH

SOC constant	ζ_p							a_π
guest species	Li[17,25]	Na[17]	K[26]	Cs[26]	Cu[27]	Ag[28]	Au[28]	NH
gas phase	0.23	11.5	38.5	369	166	614	2543	34.79
Ar	−16				124	783	3354	33.5
Kr	−70		−64		95	638	3110	21
Xe	−196	−213	−170	100−150	−23	583	2655	25.6

The trend of A_Π in Table 3 can be rationalized in terms of the external heavy-atom effect,[24] which should increase with the atomic number of the host. This effect has been investigated previously for ^{2}P terms of alkali[17,25,26] and coinage metals[27,28] trapped in noble-gas matrices by measuring MCD and absorption spectroscopy of the ^{2}P $\leftarrow$ ^{2}S transitions. In Table 4, the resultant one-electron SO coupling constants (ζ_p) of the metals are compared with the one-electron SO coupling constants ($a_\pi = |A_\Pi|$) for NH/NG. Within each metal series, the lightest atoms have ζ_p values that diminish (in comparison with the gas-phase value) on incorporation into an Ar matrix, whereas ζ_p increases for the heavier atoms. The available data suggest that both series exhibit a monotonic decrease in ζ_p as the atomic number of the matrix gas is increased.

The trends for the values of a_π of NH/Ar and NH/Kr are in keeping with those for ζ_p of the lighter metals, which is consistent with the assignment of the 1π orbitals of NH to N 2p parentage. The apparent increase from NH/Kr to NH/Xe is very possibly an artifact arising from the fact that the data for the latter were obtained in the low-field, linear limit ($\mu_B B/kT \ll 1$), where the second term in eq 7 is almost linear in the magnetic field and the $\mathscr{A}$ and $\mathscr{C}$ term contributions are more difficult to separate. Support for this conjecture is provided by an analysis of Rose's linear-limit data for NH/Ar,[8] which gives $a_\pi \approx 39$ cm^{-1}, substantially larger than the value for NH/Ar in Table 4.

For NH/N_2, $a_\pi = 43.2 \pm 0.3$ cm^{-1}, which is nearly 25% greater that the gas-phase value, suggesting that the interactions of excited-state NH radicals with N_2 molecules are substantially different from those with noble-gas atoms. In the absence of quantum mechanical calculations, we resist the temptation to speculate on the nature of these differences.

For NH/NG and NH/N_2, D' is strongly reduced in comparison with the gas-phase value of D (Table 3). The possibility that this quenching arises from guest−host SO interactions can be discounted because the SO contribution to D is only ∼12%.[29] The explanation must be that the NH molecules exercise a significant degree of orientational freedom within the matrices. For NH/NG, D' is reduced effectively to zero, which indicates that the guest radicals behave essentially as free rotors for which the lowest ($J = 1$) rotational level is necessarily triply degenerate in the absence of a magnetic field.

Because X $^3\Sigma^-$ NH behaves as a free rotor in the noble-gas matrices, the guest−host interactions must be weak. As these interactions are made stronger, the hindrance of rotational freedom should be manifest as a nonvanishing D'. N_2 is reported

to form a relatively strongly interacting matrix,[30] and in agreement with expectations, D' has increased to more than a third of the gas-phase D value.

As noted above, moment analysis reveals nothing about excited-state CF effects. In the case of NH/Ar, simulated A $^3\Pi_i \leftarrow$ X $^3\Sigma^-$ MCD and absorption spectra obtained by assuming that the excited-state SO splitting is augmented by a CF splitting of $V_0 \approx 38$ cm^{-1} were in reasonable agreement with experiment.[1] The spectra reported here are almost structureless in comparison with those of NH/Ar. Consequently, it is more difficult to obtain a uniquely good simulation, and we are not confident about the reliability of the parameters that are extracted from such a procedure. However, we do find that the better simulations are obtained with $V_0 \approx 30$ cm^{-1} for NH/Kr and $V_0 \approx 100$ cm^{-1} for NH/N_2, consistent with the conclusion that guest−host interactions are stronger in N_2 matrices than in noble-gas matrices.

V. Conclusion

Absorption and temperature- and magnetic field-dependent MCD spectra have been obtained for the A $^3\Pi_i \leftarrow$ X $^3\Sigma^-$ transitions of NH/NG and NH/N_2. The MCD spectra are dominated by pairs of $\mathscr{C}$ terms of opposite sign, giving temperature-dependent pseudo-$\mathscr{A}$ terms that exhibit saturation with respect to increasing magnetic field and decreasing temperature.

Moment analysis of the data was used to determine the SO coupling constants for the A $^3\Pi_i$ terms and ZFSs for the X $^3\Sigma^-$ terms. The one-electron SO coupling constants (a_π) show a slight decrease from the gas-phase value on incorporation into Ar, followed by further decreases with heavier noble-gas hosts. These observations are consistent with the external heavy-atom effect, as evidenced by its similarity to the behavior of the lighter alkali and coinage metals.

In noble-gas matrices, the ZFS of the lowest $^3\Sigma^-$ level of NH is reduced effectively to zero. This is consistent with the conclusion that the guest radicals are acting as free rotors, in agreement with the findings by previous workers using other spectroscopic techniques.[5,6] For NH/N_2, the quenching of D' is less severe, indicating that rotation of the guest is significantly more hindered and confirming the earlier summation that guest−host interactions in N_2 matrices are significantly greater than in noble-gas matrices.[30]

Simulations give fairly good agreements with experiment, but the model we have employed has serious weaknesses. Most importantly, it is based on an assumption that individual guest radicals have a fixed orientation on the time scale of the experiment, yet the reduced D' values are interpreted to indicate rotational freedom in the ground state. Future work will attempt to remedy this by including an explicit consideration of the dynamics and interactions within these matrices.

Acknowledgment. We are grateful to Professor Paul N. Schatz for supplying us with earlier absorption and MCD data for NH/NG. We thank the University of Canterbury for providing J.J.H. with a Doctoral Scholarship and for financially supporting this research through grant U6501.

References and Notes

(1) Langford, V. S.; Williamson, B. E. *J. Phys. Chem. A* **1998**, *102*, 2415−2423.
(2) Harrison, J. J. Ph.D. Thesis, University of Canterbury, Christchurch, New Zealand, 2003.
(3) Robinson, G. W.; McCarty, M. J. *J. Chem. Phys.* **1958**, *28*, 350.
(4) Robinson, G. W.; McCarty, M. J. *Can. J. Phys.* **1958**, *36*, 1590−1591.
(5) McCarty, M. J.; Robinson, G. W. *J. Am. Chem. Soc.* **1959**, *81*, 4472−4476.
(6) Bondybey, V. E.; Brus, L. E. *J. Chem. Phys.* **1975**, *63*, 794−804.
(7) Lund, P. A.; Hasan, Z.; Schatz, P. N.; Miller, J. H.; Andrews, L. *Chem. Phys. Lett.* **1982**, *91*, 437−439.
(8) Rose, J. L. Ph.D. Thesis, University of Virginia, Charlottesville, VA, 1987.
(9) Langford, V. S. Ph.D. Thesis, University of Canterbury, Christchurch, New Zealand, 1997.
(10) Langford, V. S.; Williamson, B. E. *J. Phys. Chem. A* **1997**, *101*, 3119−3124.
(11) Langford, V. S.; Williamson, B. E. *J. Phys. Chem. A* **1998**, *102*, 138−145.
(12) Durig, J. R.; Sullivan, J. F. In *Matrix Isolation Spectroscopy*; Barnes, A. J., Orville-Thomas, W. J., Muller, A., Gaufres, R., Eds.; D. Reidel Publishing Company: Dordrecht, The Netherlands, 1981.
(13) Dunford, C. L. Ph.D. Thesis, University of Canterbury, Christchurch, New Zealand, 1997.
(14) Dunford, C. L.; Williamson, B. E. *J. Phys. Chem. A* **1997**, *101*, 2050−2054.
(15) Durieux, M.; Rusby, R. L. *Metrologia* **1983**, *19*, 67−72.
(16) Misener, G. C. Ph.D. Thesis, University of Virginia, Charlottesville, VA, 1987.
(17) Rose, J.; Smith, D.; Williamson, B. E.; Schatz, P. N.; O'Brien, M. C. M. *J. Phys. Chem.* **1986**, *90*, 2608−2615.
(18) Krausz, E.; McDonald, P. *J. Phys. E: Sci. Instrum.* **1978**, *11*, 801−804.
(19) Krausz, E.; Mowery, R. L.; Schatz, P. N. *Ber. Bunsen-Ges. Phys. Chem.* **1978**, *82*, 134−136.
(20) Piepho, S. B.; Schatz, P. N. *Group Theory in Spectroscopy with Applications to Magnetic Circular Dichroism*; Wiley-Interscience: New York, 1983.
(21) Meyer, B. *Low-Temperature Spectroscopy*; American Elsevier Publishing Company: New York, 1971.
(22) Huber, K. P.; Herzberg, G. *Molecular Spectra and Molecular Structure*; Van Nostrand Reinhold: New York, 1979; Vol. 4.
(23) Weltner, W. J. *Magnetic Atoms and Molecules*; Dover Publications: Mineola, NY, 1989.
(24) Pellow, R.; Vala, M. *J. Chem. Phys.* **1989**, *90*, 5612−5621.
(25) Lund, P. A.; Smith, D.; Jacobs, S. M.; Schatz, P. N. *J. Phys. Chem.* **1984**, *88*, 31−42.
(26) Samet, C.; Rose, J. L.; Schatz, P. N.; O'Brien, M. C. M. *Chem. Phys. Lett.* **1989**, *159*, 567−572.
(27) Vala, M.; Zeringue, K.; ShakhsEmampour, J.; Rivoal, J.-C.; Pyzalski, R. *J. Chem. Phys.* **1984**, *80*, 2401−2406.
(28) Roser, D.; Pellow, R.; Eyring, M.; Vala, M.; Lignieres, J.; Rivoal, J.-C. *Chem. Phys.* **1992**, *166*, 393−409.
(29) Wayne, F. D.; Colbourn, E. A. *Mol. Phys.* **1977**, *34*, 1141−1155.
(30) Barnes, A. J. In *Matrix Isolation Spectroscopy*; Barnes, A. J., Orville-Thomas, W. J., Muller, A., Gaufres, R., Eds.; D. Reidel Publishing Company: Dordrecht, The Netherlands, 1981.
(31) Veseth, L. *J. Phys. B: At. Mol.* **1972**, *5*, 229−241.